Evolution of a massless scalar field in Reissner-Nordström anti–de Sitter spacetimes

B. Wang*
Instituto De Fisica, Universidade de Sao Paulo, C.P. 66.318, CEP 05315-970, Sao Paulo, Brazil and Department of Physics, Shanghai Teachers' University, People's Republic of China

C. Molina† and E. Abdalla‡
Instituto De Fisica, Universidade de Sao Paulo, C.P. 66.318, CEP 05315-970, Sao Paulo, Brazil
(Received 24 August 2000; published 27 February 2001)

We investigate the evolution of a scalar field propagating in Reissner-Nordström anti–de Sitter spacetime. Because of the characteristic of spacetime geometry, the radiative tails associated with a massless scalar field propagation have an oscillatory exponential decay. The object picture of the quasinormal ringing has also been obtained. For small charges, the approach to thermal equilibrium is faster for larger charges. However, after the black-hole charge reaches a critical value, we get the opposite behavior for the imaginary frequencies of the quasinormal modes. Some possible explanations concerning the wiggle of the imaginary frequencies have been given. The picture of the quasinormal modes depending on the multipole index has also been illustrated.

DOI: 10.1103/PhysRevD.63.084001 PACS number(s): 04.30.Nk, 04.70.Bw

I. INTRODUCTION

The study of wave dynamics outside black holes has been an intriguing subject for the last few decades (for a review, see Ref. [1]). By virtue of previous works, we now have the schematic picture regarding the dynamics of waves outside a spherical collapsing object. A static observer outside the black hole can indicate three successive stages of the wave evolution. First the exact shape of the wave front depends on the initial pulse. This stage is followed by a quasinormal ringing, which carries information about the structure of the background spacetime and is believed to be a unique fingerprint to directly identify the black hole's existence. Detection of these quasinormal modes is expected to be realized through gravitational wave observation in the near future [1]. Finally, at late times, quasinormal oscillations are swamped by the relaxation process. This relaxation is the requirement of the black hole no-hair theorem [2]. In addition, the dynamical mechanism of shedding the perturbation hair near the black hole event horizon is of direct interest to the problem of stability of Cauchy horizons [3].

The mechanism responsible for the relaxation of neutral external perturbations was first exhibited by Price [4]. Studying the behavior of a massless scalar field propagating on a fixed Schwarzschild background, he showed that for a fixed position the field dies off with a power-law tail. The behavior of neutral perturbations along null infinity and a future event horizon was further studied by Gundlach, Price, and Pullin [5] and similar power-law tails have been obtained. These results were later confirmed using several different techniques, both analytic and numerical [6–8], and were generalized to Reissner-Nordström (RN) background [5,9]. The application of linear approaches is encouraged by numerical analysis of the fully nonlinear dynamics of the fields [10,11], which indicates the same late time pattern of decay.

Extending the basic scenario to study the asymptotic evolution of charged fields and self-interacting massive scalar field around a RN black hole, Hod and Piran [12,13] found that although usual inverse power-law relations of these fields present at timelike infinity and null infinity, along the future black-hole event horizon this power-law tail is accompanied by an oscillatory behavior. Recently, Brady *et al.* [14,15] studied scalar wave dynamics in nonasymptotically flat exteriors of Schwarzschild–de Sitter and RN de Sitter black holes. Contrary to the asymptotically flat geometries, no power-law tails were detected in these cases. Instead the waves were found to decay exponentially at late times. For $l=0$, they found that the field does not decay, but settles down to a nonzero constant. Moreover, for a field strongly coupled to curvature, they obtained that the wave function oscillates with an exponentially decaying amplitude. These observations support the earlier argument by Ching *et al.* [16], that usual inverse power-law tails, as seen in asymptotically flat black hole spacetimes, are not a general feature of wave propagation in curved spacetime. Besides some relation to the perturbative field, the relaxation process reflects a characteristic of the background geometry.

It is of interest to extend this study to anti–de Sitter (AdS) spacetime. In addition to three major aspects that the evolution of test field is associated with, including the no-hair theorem, the stability of Cauchy horizon, and direct evidence of the existence of black hole provided by quasinormal ringing, the recent discovery of the anti–de Sitter–conformal-field-theory (AdS/CFT) correspondence makes the investigation in AdS black-hole background more appealing. The quasinormal frequencies of AdS black hole have direct interpretation in terms of the dual CFT. In terms of the AdS/CFT correspondence [17–19a], the black hole corresponds to an approximately thermal state in the field theory, and the decay of the test field corresponds to the decay of the perturbation of the state. The first study of the scalar quasinormal modes in AdS space was performed by Chan and Mann [19b]. In [19c], topological black holes were included. Recently,

*Email address: binwang@fma.if.usp.br
†Email address: cmolina@fma.if.usp.br
‡Email address: eabdalla@fma.if.usp.br

Horowtiz and Hubeny [20] considered the problem of quasinormal modes on the background of Schwarzschild AdS black holes in four, five, and seven dimensions. They claimed that for large black holes both the real and imaginary parts of the quasinormal frequencies scale linearly with the black-hole temperature. The time scale for approaching the thermal equilibrium is detected by the imaginary part of the lowest quasinormal frequency and is proportional to the inverse of the black-hole temperature. Considering that the RN AdS solution provides a better framework than the Schwarzschild AdS geometry and may contribute significantly to our understanding of space and time, we generalized the study made in our previous work [22]. We found that the charge in RN AdS black hole showed a richer physics concerning quasinormal modes and further information on AdS/CFT correspondence. The bigger the black hole charge is, the quicker for their approach to thermal equilibrium in CFT. However these studies focused much on frequencies of the quasinormal modes, the object picture of the evolution of test field around the AdS background is lacking.

The intention of this paper is to analyze in detail the wave propagation of massless scalar field in RN AdS spacetime. We will show that the direct picture of the evolution presents us with a perfect agreement on quasinormal frequencies with those obtained by using approximation method suggested in Ref. [20]. Moreover, our paper will show object pictures of the behavior of quasinormal modes as a function of the charge Q and of the multipole order of the field l. We will also address some discussions on the highly charged background case. In addition, the relaxation process at the event horizon will also be discussed in our direct picture. We found that the decay has the pattern of oscillatory exponential tail. This result supports Horowitz's claim that there are no power-law tails at late times in AdS space. Some physical explanation related to this result will be given.

II. EQUATIONS AND NUMERICAL METHODS

The Reissner-Nordström black-hole solution of Einstein's equations in free space with a negative cosmological constant $\Lambda=-3/R^2$ is given by

$$ds^2=-h dt^2+h^{-1}dr^2+r^2 d\Omega^2, \tag{1}$$

with

$$h=1-\frac{r_+}{r}-\frac{r_+^3}{R^2 r}-\frac{Q^2}{r_+ r}+\frac{Q^2}{r^2}+\frac{r^2}{R^2}. \tag{2}$$

The asymptotic form of this spacetime is AdS. The mass of the black hole is

$$M=\frac{1}{2}\left(r_+ +\frac{r_+^3}{R^2}+\frac{Q^2}{r_+}\right). \tag{3}$$

The Hawking temperature is given by the expression

$$T_H=\frac{1-\frac{Q^2}{r_+^2}+\frac{3r_+^2}{R^2}}{4\pi r_+} \tag{4}$$

and the potential by

$$\phi=\frac{Q}{r_+}. \tag{5}$$

In the extreme case r_+ and Q satisfy the relation

$$1-\frac{Q^2}{r_+^2}+\frac{3r_+^2}{R^2}=0. \tag{6}$$

For a nonextreme RN AdS black hole, the spacetime possesses two horizons, namely, the black-hole event horizon r_+ and Cauchy horizon r_-. For the extreme case where Eq. (6) is satisfied, these two horizons degenerate. The function h has four zeros at r_+, r_- and r_1, r_2, where r_1, r_2 are two complex roots with no physical meaning. The relations between these four roots are

$$\begin{aligned} r_1+r_2&=-(r_+ +r_-)\\ r_1 r_2&=R^2+r_+ r_- +r_+^2+r_-^2. \end{aligned} \tag{7}$$

In terms of these quantities, h can be expressed as

$$h=\frac{1}{R^2 r^2}(r-r_+)(r-r_-)(r-r_1)(r-r_2). \tag{8}$$

Introducing the surface gravity κ_i associated with r_i by the relation $\kappa_i=\frac{1}{2}|dh/dr|_{r=r_i}$, we have

$$\begin{aligned} \kappa_{r_+}&=\frac{1}{2R^2}\frac{(r_+-r_-)(r_+-r_1)(r_+-r_2)}{r_+^2},\\ \kappa_{r_-}&=\frac{1}{2R^2}\frac{(r_+-r_-)(r_--r_1)(r_--r_2)}{r_-^2},\\ \kappa_{r_1}&=\frac{1}{2R^2}\frac{(r_+-r_1)(r_--r_1)(r_1-r_2)}{r_1^2},\\ \kappa_{r_2}&=\frac{1}{2R^2}\frac{(r_+-r_2)(r_--r_2)(r_2-r_1)}{r_2^2}. \end{aligned} \tag{9}$$

These quantities allow us to write

$$\begin{aligned} h^{-1}=&\frac{1}{2\kappa_{r_+}(r-r_+)}-\frac{1}{2\kappa_{r_-}(r-r_-)}+\frac{1}{2\kappa_{r_1}(r-r_1)}\\ &-\frac{1}{2\kappa_{r_2}(r-r_2)}. \end{aligned} \tag{10}$$

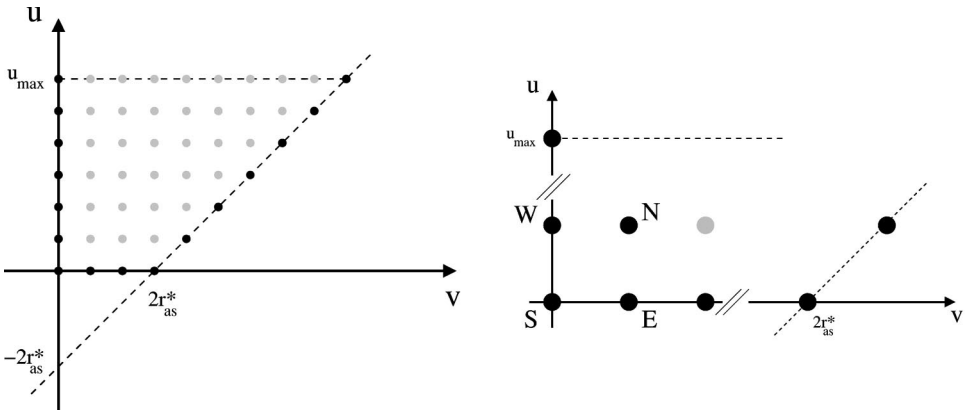

FIG. 1. (Left) Diagram of the numerical grid and the domain of interest. The black spots represent the grid points where the value of the field is known. The gray spots represent the grid points to be calculated. The points in the line $u=u_{max}$ are the results shown in this paper. (Right) Detail of the previous diagram, showing the relative positions *N*, *S*, *E*, and *W*. The gray point would be the next one to be calculated.

Combining the last two terms in Eq. (10), we express the transformation between r and the ''tortoise coordinate'' $r^*=\int h^{-1}dr$ in the form

$$r^*=\frac{1}{2\kappa_{r_+}}\ln(r-r_+)-\frac{1}{2\kappa_{r_-}}\ln(r-r_-)+\frac{R^2[(r_1r_2)^2-r_+r_-r_1r_2]}{[r_+^2-r_+(r_1+r_2)+r_1r_2][r_-^2-r_-(r_1+r_2)+r_1r_2]}\times\int\frac{dr}{r^2-r(r_1+r_2)+r_1r_2}+\frac{R^2[r_+r_-(r_1+r_2)-r_+r_1r_2-r_-r_1r_2]}{[r_+^2-r_+(r_1+r_2)+r_1r_2][r_-^2-r_-(r_1+r_2)+r_1r_2]}\times\int\frac{r\,dr}{r^2-r(r_1+r_2)+r_1r_2}. \tag{11}$$

In terms of t and r^* we introduce null coordinates $u=t-r^*$ and $v=t+r^*$ so that the future black-hole horizon is located at $u=\infty$. Since the quasinormal modes of AdS space are defined to be modes with only ingoing waves near the horizon, we will pay more attention to the wave dynamics near the event horizon.

Let us consider a massless scalar field Φ in the RN AdS spacetime, obeying the wave equation

$$\Box\Phi=0, \tag{12}$$

where $\Box=g^{\alpha\beta}\nabla_\alpha\nabla_\beta$ is the d'Alembertian operator. If we decompose the scalar field according to

$$\Phi=\sum_{lm}\frac{1}{r}\psi_l(t,r)Y_{lm}(\theta,\phi) \tag{13}$$

then each wave function $\psi_l(r)$ satisfies the equation

$$-\frac{\partial^2\psi_l}{\partial t^2}+\frac{\partial^2\psi_l}{\partial r^{*2}}=V_l\psi_l, \tag{14}$$

where

$$V_l=h\left[\frac{l(l+1)}{r^2}+\frac{1}{r}\frac{dh}{dr}\right]=h\left[\frac{l(l+1)}{r^2}+\frac{r_++r_+^3/R^2+Q^2/r_+}{r^3}-\frac{2Q^2}{r^4}+\frac{2}{R^2}\right]. \tag{15}$$

The potential V_l has the same characteristic as that in the Schwarzschild AdS black hole. It is positive and vanishes at the horizon, but diverges at $r\to\infty$, which requires that Φ vanishes at infinity. This is the boundary condition to be satisfied by the wave equation for the scalar field in AdS space. In terms of the radial coordinate r^*, it is seen that when r tends to infinity, r^* tends to a finite constant (which we denote r^*_{as}). It means that our region of interest in the $(u-v)$ diagram is above the line $v-u=2r^*_{as}$, as shown in Fig. 1. In this line (where $r\to\infty$) we set $\Phi=0$.

The behavior of the potential differs quite a lot from that of asymptotically flat space and de Sitter space. As argued in Ref. [16], it is this peculiarity that contributes to the special wave propagation as will be shown later.

Using the null coordinates u and v, Eq. (14) can be recast as

$$-4\frac{\partial^2}{\partial u\,\partial v}\psi_l(u,v)=V_l(r)\psi_l(u,v) \tag{16}$$

in which r is determined by inverting the relation $r^*(r)=(v-u)/2$.

The two-dimensional wave equation (16) can be integrated numerically, using for example the finite difference method suggested in Refs. [5,21]. Using Taylor's theorem, it is discretized as

$$\psi_N=\psi_E+\psi_W-\psi_S-\delta u\,\delta v\,V_l\left(\frac{v_N+v_W-u_N-u_E}{4}\right)\frac{\psi_W+\psi_E}{8}+\mathcal{O}(\epsilon^4), \tag{17}$$

where the points N,S,E, and W form a null rectangle with relative positions as $N{:}(u+\delta u,v+\delta v)$, $W{:}(u+\delta u,v)$, $E{:}(u,v+\delta v)$, and $S{:}(u,v)$. The parameter ϵ is an overall grid scalar factor, so that $\delta u\sim\delta v\sim\epsilon$.

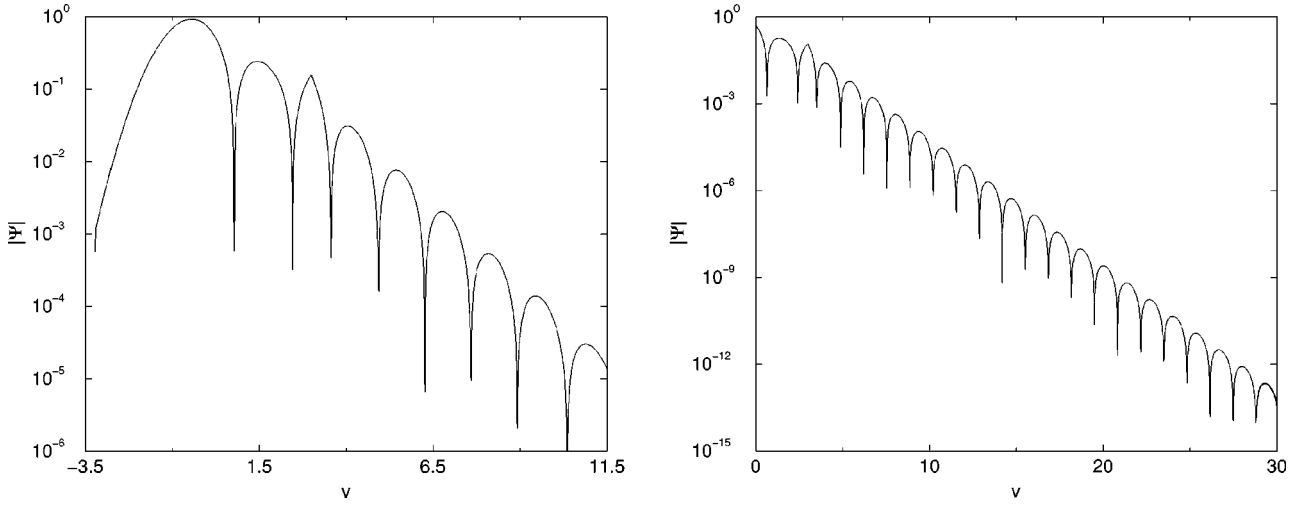

FIG. 2. Semilog graph of the absolute value of the wave function for small values of v (left) and the late time behavior (right), with $r_+=0.4$ and $Q=0$.

Considering that the behavior of the wave function is not sensitive to the choice of initial data, we set $\psi_l(u,v=v_0)=0$ and use a Gaussian pulse as an initial perturbation, centered on v_c and with width σ on $u=u_0$ as

$$\psi_l(u=u_0,v)=\exp\left[-\frac{(v-v_c)^2}{2\sigma^2}\right]. \tag{18}$$

The inversion of the relation $r^*(r)$ needed in the evaluation of the potential $V_l(r)$ is the most tedious part in the computation. We overcome this difficulty by employing the method suggested in Refs. [5,14].

After the integration is completed, the value $\psi_l(u_{max},v)$ is extracted, where u_{max} is the maximum value of u on the numerical grid. Taking sufficiently large u_{max}, $\psi_l(u_{max},v)$ represents a good approximation for the wave function at the event horizon $(u\to\infty)$, which carries information about the quasinormal modes for the AdS space of our interest. It was observed in our numerical experiments that the plots obtained converged in a given range of v, as expected, but the rate of convergence varied with the parameters of the system. It should be noted that the term ''convergence'' in the last sentence refers to the limit of Φ as u_{max} is taken bigger and bigger. As commented, the region $u_{max}\to\infty$ corresponds to the event horizon, in which we are interested. Some comments about the convergence of the numerical code, meaning the evolution of the wave function with the grid size, is made in Appendix. In order to compare our results here with those in Refs. [20,22], we fix $R=1$ in the following.

III. NUMERICAL RESULTS

We now report on the results of our numerical simulations of evolving massless scalar field on a RN AdS black-hole background. Taking $Q\to 0$, our results reflect the properties on Schwarzschild AdS background.

A. Behavior of wave evolution for $l=0$

In the first series of numerical experiments, we choose the multipole index $l=0$ and examine the behavior of the test-field propagation with the increase of the charge of the background spacetime.

Figure 2 displays the quasinormal ringing on the 4D Schwarzschild-AdS background. From plots using different values of r_+ we can read off values for the imaginary (ω_I) and real (ω_R) parts of the frequency. The results are shown in Table I.

The agreement with the frequencies calculated in Ref. [20] is good. A small difference can be attributed to the different methods employed.

We studied the late-time decay of the test field on the Schwarzschild-AdS black hole and the results are shown in Fig. 2. It was first predicted in Ref. [20] that the decay is always exponential and with no power-law tails. Through careful study, we got a result that supports their claim. We obtain that the late-time falloff is oscillatory exponential. Recall that for the AdS black hole, the potential diverges at infinity but vanishes exponentially near the black-hole horizon. This boundary condition differs completely from that of asymptotically flat spacetime. Using the argument of Ching

TABLE I. The lowest quasinormal mode frequency for four-dimensional Schwarzschild-AdS black hole for $l=0$. The real part is ω_R^1 and the imaginary part is ω_I^1.

r_+	ω_I^1	ω_R^1
100	274.61	185.38
50	133.68	91.38
10	26.79	18.85
5	13.41	9.99
1	2.67	2.79
0.8	2.15	2.58
0.6	1.58	2.41
0.4	1.006	2.362

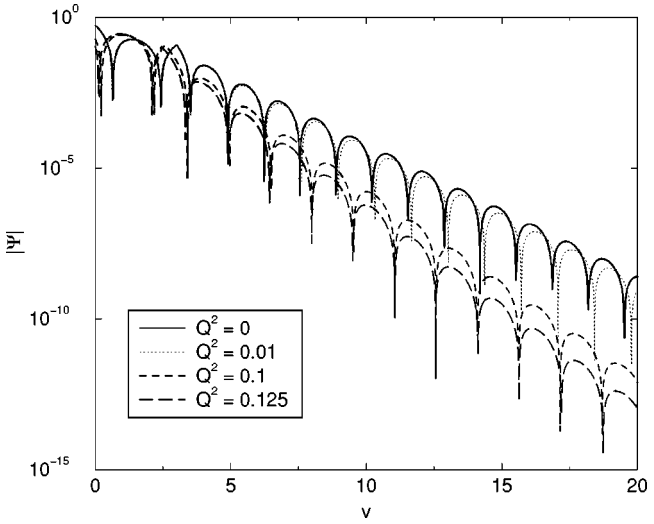

FIG. 3. Semilog graphs of $|\Psi|$ with $r_+ = 0.4$ and small values of Q. The extreme value for Q^2 is 0.2368.

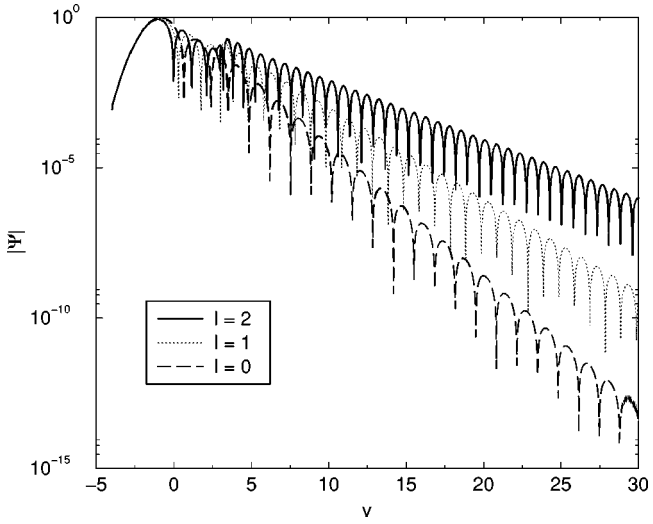

FIG. 4. Semilog graph of the wave function in the $Q=0$ case for $r_+ = 0.4$, with $l = 0,1,2$.

et al. [16], it is not difficult to understand the reason that the usual power-law tail is replaced by exponential decay. Since that potential also falls off exponentially on the black-hole horizon in de Sitter space, the pattern of decay exhibited here on the AdS black-hole event horizon is similar to that in de Sitter space [14,15]. However due to the waves bouncing off the divergent potential barrier at large r in AdS space, the oscillation appears in the exponential tail. With the late-time behavior in hand, it is possible to improve previous studies on Cauchy horizon stability problems in AdS black holes [23,24] along the lines of Brady and Smith [25].

Figure 3 demonstrates the behaviors of the field with the increase of the charge in the RN AdS black-hole background. In Table II we listed values of imaginary and real parts of quasinormal frequencies read from the plots. These frequencies together with the entire picture presented in Fig. 3 agree perfectly with the result given in Ref. [22], since the imaginary and real parts of the quasinormal frequencies relate to the damping time scale ($\tau_1 = 1/\omega_i$) and oscillation time scale ($\tau_2 = 1/\omega_r$), respectively. We learned that as Q increases, ω_i increases as well, which corresponds to the decrease of the damping time scale. According to the AdS/CFT correspondence, this means that for bigger Q, it is quicker for the quasinormal ringing to settle down to thermal equilibrium. From Fig. 3 it is easy to see this property. Besides, Table II and Fig. 3 also tell us that the bigger Q is, the lower frequencies of oscillation will be. This object picture supports the argument in Ref. [22] that if we perturb a RN AdS black hole with high charge, the surrounding geometry will not ''ring'' as much and as long as that of the black hole with small Q. It is easy for the perturbation on the high charged AdS black-hole background to return to thermal equilibrium. However this relation seems not to hold well when the charge is sufficiently big and near the extreme value described by relation (6). We will address this behavior later.

TABLE II. The behavior of the lowest quasinormal mode frequency with the increase of the charge in the RN AdS black-hole background for $l=0$. The real part is ω_R^1 and the imaginary part is ω_I^1.

	$r_+ = 0.4$ $(Q^2_{ext} = 0.2368)$		
Q^2	r_-	ω_I^1	ω_R^1
0	0	1.007	2.363
0.01	2.14E-2	1.034	2.327
0.1	0.196	1.42	2.05
0.125	0.238	1.53	2.04
	$r_+ = 1$ $(Q^2_{ext} = 4)$		
Q^2	r_-	ω_I^1	ω_R^1
0	0	2.67	2.79
0.01	4.9875E-003	2.68	2.78

B. Behavior of wave evolution with the increase of *l*

We have so far discussed only the lowest multipole index $l=0$. In the following we show the wave dynamics on the RN AdS background for different multipole indices l. For simplicity we present here the results for $l=0,1,2$, but the basic characteristics of the dependence of the wave function with the multipole index have already been uncovered and are discussed in this section.

Figures 4–6 exhibit a striking consistent picture with those given in Refs. [20,22]. Increasing l, the evolution of the test field experiences an increase of the damping time scale and a decrease of the oscillation time scale. These figures gave us an object lesson on the evolution of the test field with the increase of multipole index. It is worth noting that the behavior shown here differs quite a lot from that of the asymptotically flat case [5], where the perturbation settles down faster with the increase of l. These differences can be used to further support the argument that the last two processes of the wave evolution reflect directly on the background spacetime property.

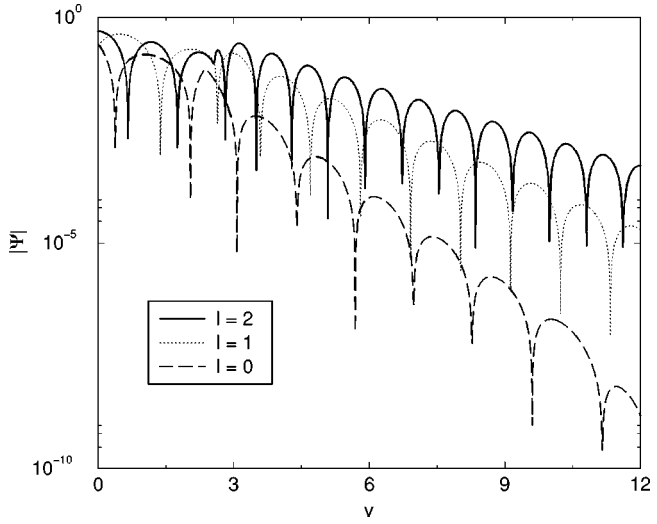

FIG. 5. Semilog graph of the wave function for $Q^2=0.1$ and $r_+=0.4$, with $l=0,1,2$.

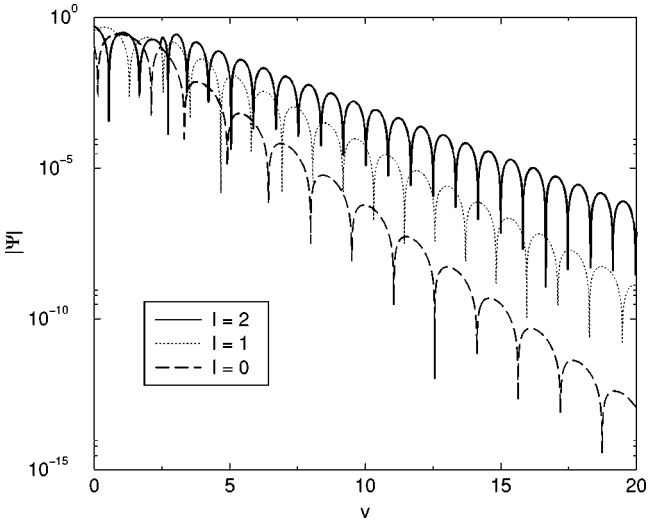

FIG. 6. Semilog graph of the wave function for $Q^2=0.125$ and $r_+=0.4$, with $l=0,1,2$.

C. Quasinormal modes for highly charged AdS black hole

In our previous work [22], we found that there is a numerical convergence problem when the charge Q approaches the extreme value. We claimed that the problem is related to the method we adopted there. Using the numerical strategy proposed in Ref. [5] to directly describe the wave dynamics, we can step further on this problem.

The behavior we read from Fig. 7 is quite different from that exhibited in Fig. 3 and discussed in Sec. III A. Here we see that over some critical value of Q, the damping time scale increases with the increase of Q, corresponding to the decrease of imaginary frequency. This means that over some critical value of Q, the larger the black-hole charge is, the slower the outside perturbation dies out. This qualitative change in the characteristic of the imaginary frequency as Q increases agrees with the normal-mode frequencies of RN black hole described in Refs. [26,27].

We found in the numerical calculation that the computation time becomes bigger when Q is large enough. This happens because we are forced to take a bigger u_{max}, and also because the numerical routine that calculates the function $r(r^*)$ is more time consuming in this range of Q. Moreover, the precision cannot be improved for taking smaller grid scale factor when Q is close to the extreme value. Some plateaus appear in the late time leading us to suspect that there may be a failure in the numerical method in this region. In spite of this, the convergence of the numerical code appears to be good even in this limit, as commented in Appendix. However the question whether there is a plausible explanation for the ''wiggle'' of the imaginary frequency as the charge is large enough and close to the extreme value is still open.

We know that the frequencies and damping times of the quasinormal modes are entirely fixed by the black hole, and are independent of the initial perturbation. It has been shown

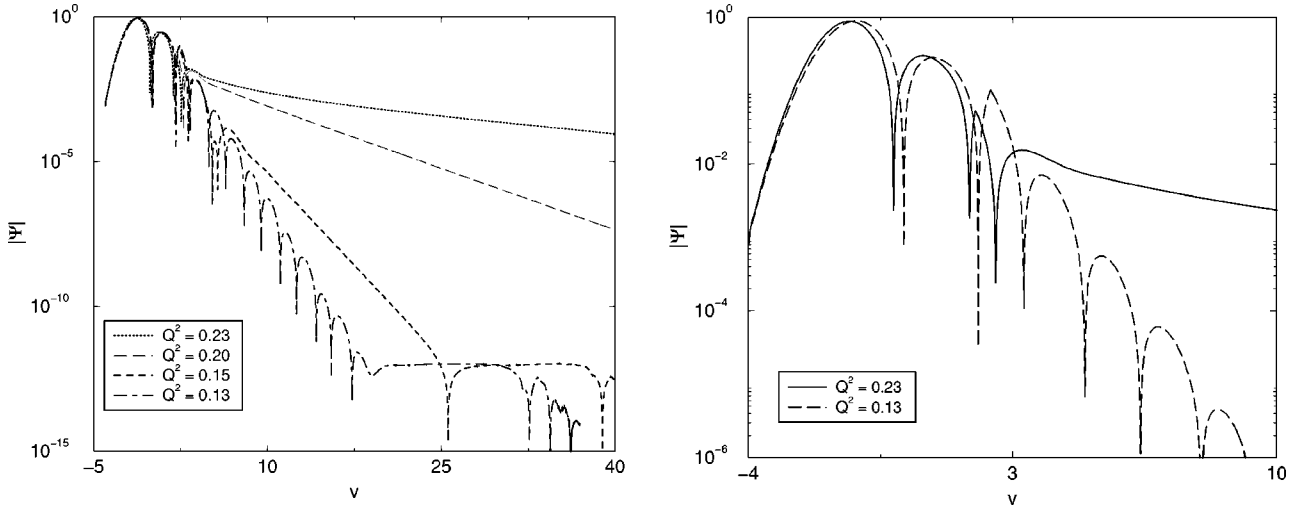

FIG. 7. (left) Semilog graph of the wave function with $r_+=0.4$, $l=0$, and several values of Q. The extreme value for Q^2 is 0.2368. (right) Detail of previous plot, with two values of Q.

that there is a second-order phase transition in the extreme limit of black holes [28–30]. This result has been further supported in a recent study for the charged AdS black hole [31,32]. Whether different properties of imaginary frequencies with the increase of the charge Q reflect different phase characteristics is a question to be answered. We are trying to improve our numerical code to increase convergence rate and precision. These results can be compared to those of Ref. [33] where it has been shown that in the Kerr solution, when the rotation parameter a of the black hole approaches the critical value, the quasinormal modes decay time gets longer. These results support the claims of the present paper. We will address this problem in detail in a forthcoming paper.

IV. CONCLUSIONS AND DISCUSSIONS

We have studied the wave evolution in Reissner-Nordström anti–de Sitter spacetimes and revealed consistent but interesting results. The radiative tails associated with a massless scalar field propagation on a fixed background of an AdS black hole experience an oscillatory exponential decay at the black-hole event horizon. This result of exponential decay supports Ref. [20] and is similar to that on the black-hole horizon in de Sitter case because of the similar behavior of the exponentially falling off of the potential at event horizon. When one considers the conclusions of Ching *et al.* [16], this late-time tail is not surprising. Accompanied with the exponentially decay, there is a special oscillation in the tail in linear analysis in AdS. This can be attributed to waves bouncing off the potential at large r, because the potential diverges at infinity in AdS space. The property of the late-time behavior on the event horizon of AdS black hole can help us better understand the stability of Cauchy horizon in AdS spacetimes.

We have also learned an object lesson of the quasinormal modes on the background of RN AdS black hole. For small values of Q the picture we obtained is consistent with that derived in Ref. [22]. The larger the black hole charge is, the quicker is the approach to thermal equilibrium. The consistent picture of the quasinormal modes, depending on the multipole index l, has also been illustrated. Increasing l, we obtain the effect of increasing the damping time scale and decreasing the oscillation time scale.

When the charge in background RN AdS black hole is large enough, we get an opposite result for the characteristic of imaginary frequencies. This wiggle of the imaginary frequencies as the charge increases on the background agrees with earlier results of normal-mode frequency study for RN black hole. Since the type of quasinormal mode is determined by the background spacetimes and it has been found that a second-order phase transition appears when the RN AdS black hole becomes extreme, we speculate that the different behavior of the quasinormal frequencies may reflect the characteristic of two different phases. Further study on this subject is called for.

ACKNOWLEDGMENTS

This work was partially supported by Fundação de Amparo à Pesquisa do Estado de São Paulo (FAPESP) and Conselho Nacional de Desenvolvimento Científico e Tecnológico (CNPQ). B. Wang would like to acknowledge the support given by Shanghai Science and Technology Commission, as well as NNSF, China under Contract 10005004.

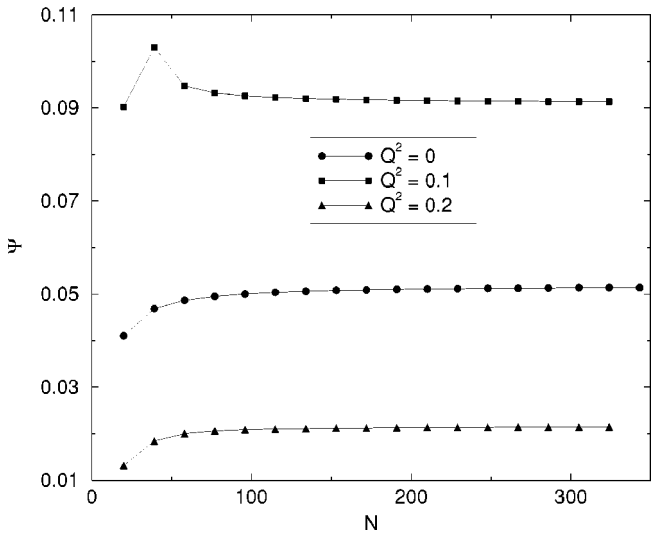

FIG. 8. Graph of Ψ_l for $v=2.9824$, $r_+=0.4$, $l=0$, and several values of Q.

APPENDIX: CONVERGENCE OF THE CODE

As shown in expression (17), the local truncation error for Ψ_N scales as ϵ^4, assuming that the exact function Ψ_l has a Taylor expansion in the null rectangle. Although we have little control over the global error at $u=u_{max}$, we can make a rough estimate. The first point in the line $u=u_{max}$, which is $\Psi(u_{max},v_1)$, is obtained using only points in the line $v=v_1$. Since there are $\mathcal{O}(\epsilon^{-1})$ points in this line, the global error in $\Psi_l(u_{max},v_1)$ should scale as ϵ^3. On the other hand, since there are $\mathcal{O}(\epsilon^{-2})$ grid points, the last point in the line $u=u_{max}$, which depends on all the grid points, should scale as ϵ^2.

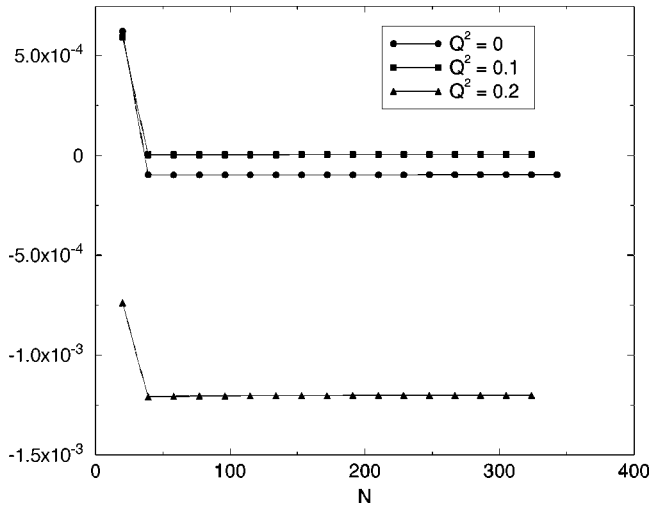

FIG. 9. Graph of Ψ_l for $v=9.6157$, $r_+=0.4$, $l=0$, and several values of Q.

We can improve on this estimate by calculating convergence curves. In these curves, we plot the value of Ψ_l at a given point as the grid spacing ϵ is reduced. In Figs. 8 and 9 we show some curves for three values of the charges in two points. The parameter N is the number of points in the line $u=u_0$. It is therefore inversely proportional to ϵ.

These diagrams clearly show numerical convergence, and a quite fast one. This indicates that the global error indeed tends to zero as we decrease the grid spacing, even in the limit when Q gets near the extreme limit.

[1] K. D. Kokkotas and B. G. Schmidt, gr-qc/9909058, and references therein.

[2] C. W. Misner, K. S. Thorne, and J. A. Wheeler, *Gravitation* (Freeman, San Franciso, 1973).

[3] E. Poisson and W. Israel, Phys. Rev. D **41**, 1796 (1990).

[4] R. H. Price, Phys. Rev. D **5**, 2419 (1972); **5**, 2439 (1972).

[5] C. Gundlach, R. H. Price, and J. Pullin, Phys. Rev. D **49**, 883 (1994).

[6] R. Gomez, J. Winicour, and B. G. Schmidt, Phys. Rev. D **49**, 2828 (1994).

[7] E. Leaver, J. Math. Phys. **27**, 1238 (1986); Phys. Rev. D **34**, 384 (1986).

[8] N. Andersson, Phys. Rev. D **55**, 468 (1997).

[9] J. Bicak, Gen. Relativ. Gravit. **3**, 331 (1972).

[10] C. Gundlach, R. H. Price, and J. Pullin, Phys. Rev. D **49**, 890 (1994).

[11] L. M. Burko and A. Ori, Phys. Rev. D **56**, 7820 (1997).

[12] S. Hod and T. Piran, Phys. Rev. D **58**, 024017 (1998).

[13] S. Hod and T. Piran, Phys. Rev. D **58**, 044018 (1998).

[14] P. R. Brady, C. M. Chambers, W. G. Laarakkers, and E. Poisson, Phys. Rev. D **60**, 064003 (1999).

[15] P. R. Brady, C. M. Chambers, W. Krivan, and P. Laguna, Phys. Rev. D **55**, 7538 (1997).

[16] E. S. C. Ching, P. T. Leung, W. M. Suen, and K. Young, Phys. Rev. D **52**, 2118 (1995); Phys. Rev. Lett. **74**, 2414 (1995).

[17] J. M. Maldacena, Adv. Theor. Math. Phys. **2**, 231 (1998).

[18] E. Witten, Adv. Theor. Math. Phys. **2**, 253 (1998).

[19] (a) S. S. Gubser, I. R. Klebanov, and A. M. Polyakov, Phys. Lett. B **428**, 105 (1998); (b) J. S. F. Chan and R. B. Mann, Phys. Rev. D **55,** 7546 (1997); (c) **59,** 064025 (1999).

[20] G. T. Horowitz and V. E. Hubeny, Phys. Rev. D **62**, 024027 (2000); G. T. Horowitz, Class. Quantum Grav. **17**, 1107 (2000).

[21] R. Gómez, J. Winicour, and R. Isaacson, J. Comp. Physiol. **98**, 11 (1992).

[22] B. Wang, C. Y. Lin, and E. Abdalla, Phys. Lett. B **481**, 79 (2000).

[23] T. M. Helliwell and D. A. Konkowskii, Phys. Rev. D **51**, 5517 (1995); **54**, 7898 (1996).

[24] B. Wang and R. K. Su, Phys. Rev. D **53**, 1950 (1996).

[25] P. R. Brady and J. D. Smith, Phys. Rev. Lett. **75**, 1256 (1995).

[26] N. Andersson, Proc. R. Soc. London **A442**, 427 (1993).

[27] K. D. Kokkotas and B. F. Schutz, Phys. Rev. D **37**, 3378 (1988).

[28] C. O. Lousto, Phys. Rev. D **51**, 1733 (1995).

[29] O. Kaburaki, Phys. Lett. A **217**, 316 (1996).

[30] R. K. Su, R. G. Cai, and P. K. N. Yu, Phys. Rev. D **50**, 2932 (1994); **48**, 3473 (1993); **52**, 6186 (1995); B. Wang and J. M. Zhu, Mod. Phys. Lett. A **10**, 1269 (1995).

[31] A. Chamblin, R. Emparan, C. V. Johnson, and R. C. Myers, Phys. Rev. D **60**, 064018 (1999).

[32] A. Chamblin, R. Emparan, C. V. Johnson, and R. C. Myers, Phys. Rev. D **60**, 104026 (1999).

[33] N. Andersson and K. Glampedakis, Phys. Rev. Lett. **84**, 4537 (2000).